Vol. 23(2) : 141~160 | Ocean and Polar Research | June 2001

Kuroshio Observation Program: Towards Real-Time Monitoring the Japanese Coastal Waters

Alexander Ostrovskii[1], Arata Kaneko[1,2], Alice Stuart-Menteth[3], Kensuke Takeuchi[1], Toshio Yamagata[4,5], Jae-Hun Park[1], Xiao Hua Zhu*[1], Noriaki Gohda[2], Hiroshi Ichikawa[6], Kaoru Ichikawa[1,7], Atsuhiko Isobe[7], Masanori Konda[1,8], and Shin-Ichiro Umatani[7]

[1]*Frontier Observational Research System for Global Change*
2-15 Natsushima-cho, Yokosuka-city, Kanagawa 237-0061, Japan
[2]*Graduate School of Engineering, Hiroshima University*
1-4-1 Kagamiyama, Higashi-Hiroshima, Hiroshima 739-8527, Japan
[3]*Southampton Oceanography Centre, University of Southampton, Waterfront Campus*
European Way, Southampton SO14 3ZH, United Kingdom
[4]*Department of Earth and Planetary Science, Graduate School of Science, Tokyo University*
7-3-1 Hongo, Bunkyo-ku, Tokyo 113-0033, Japan
[5]*Frontier Research System for Global Change*
3173-25 Showa-machi, Kanazawa-ku, Yokohama 236-0001, Japan
[6]*Division of Environment and Information Science, Faculty of Fisheries, Kagoshima University*
4-50-20 Shimoarata, Kagoshima 890-0056, Japan
[7]*Research Institute for Applied Mechanics, Kyushu University*
Kasuga, Fukuoka 816-8580, Japan
[8]*Department of Geophysics, Graduate School of Science, Kyoto University*
Kyoto 606-8502, Japan

Abstract : The challenge of predicting the Japanese coastal ocean motivated Frontier Observational Research System for Global Change (FORSGC) and the Japan Marine Science and Technology Center (JAMSTEC) to start a multiyear observational programme in the upstream Kuroshio in November 2000. This field effort, the Kuroshio Observation Program (KOP), should enable us to determine the barotropic and baroclinic components of the western boundary current system, thus, to better understand interactions of the currents with mesoscale eddies, the Kuroshio instabilities, and path bimodality. We, then, will be able to improve modeling predictability of the mesoscale, seasonal, and inter-annual processes in the midstream Kuroshio near the Japanese main islands by using this knowledge. The KOP is focused on an enhanced regional coverage of the sea surface height variability and the baroclinic structure of the mainstream Kuroshio in the East China Sea, the Ryukyu Current east of the Ryukyu's, and the Kuroshio recirculation. An attractive approach of the KOP is a development of a new data acquisition system via acoustic telemetry of the observational data. The monitoring system will provide observations for assimilation into extensive numerical models of the ocean circulation, targeting the real-time monitoring of the Japanese coastal waters.

Key words : KOP, Kuroshio, Ryukyu Current, PIES, monitoring system.

* Corresponding author. E-mail : xhzhu@jamstec.go.jp

1. Introduction

Motivation

Recent progresses in understanding the seasonal variability of the Kuroshio current system have mainly come from numerical simulations rather than observations (Sakamoto and Yamagata 1996; Kagimoto and Yamagata 1997). By using the high-resolution Princeton Ocean Model (POM), Kagimoto and Yamagata (1997) have shown, contrary to what could be expected from the Sverdrup balance, that the Kuroshio transport undergoes little seasonal change in the East China Sea (ECS). According to Kutsuwada and Teramoto (1987), the interior Sverdrup transport at 26-28° N, estimated from monthly maps of surface wind stress fields over the North Pacific during 1961-1984, has an annual cycle with a maximum value of 90.2 Sv (1 Sv $\equiv 10^6$ m^3/s) in February and a minimum value of 20.4 Sv in September. The POM showed, however, that although the Sverdrup balance is valid in the broad interior, including the Philippine Basin, the theory fails to predict the annual variation as well as winter transport of the mainstream Kuroshio south of Japan due to the existence of the Kuroshio recirculation.

The above discrepancy between the Sverdrup theory and the POM simulation was studied by analyzing the torque balance (Kagimoto and Yamagata 1997). The modeled Kuroshio transport is much smaller than that theoretically predicted for the winter monsoon season, which is characterized by a strong negative wind stress curl south of Japan. This is because topographic control prevents the western boundary current from intruding west of the Ryukyu Ridge, into the ECS. The deep northeastward flow east of the Ryukyu's, the Ryukyu Current, partly originates from a branch of the Kuroshio near Taiwan (Yang *et al.* 1999) and flows along the eastern side of the Ryukyu Islands (Worthington and Kawai 1972; Yuan *et al.* 1995, 1998). It is dominated by the barotropic component and interacts with the continental slope thereby extracting cyclonic vorticity from the rotating earth. Consequently the transport by the modeled Kuroshio in winter is much smaller than that expected from the Sverdrup theory. In other words, the topographic beta-effect constrains the Kuroshio transport.

It is important that POM simulations agree with estimates of the geostrophic transport based on hydrographic surveys along PN-line, northwest of Okinawa Island. It is also important that the model Kuroshio current structure is similar to that inferred from the acoustic Doppler velocity observations (Kaneko *et al.* 1992, 1993) and that the model successfully reproduces a basic structure of the Kuroshio as observed by Imawaki *et al.* (1997) south of Shikoku.

Nevertheless, there are still discrepancies between the model-derived circulation and the observations. Firstly, while POM predicted a large annual cycle of the total transport from the sea surface to the bottom across the ASUKA line, no apparent seasonal signal was found in the ASUKA direct current measurements combined with hydrographic data and TOPEX/POSEIDON sea surface height observations during 1992-99 (Imawaki *et al.* 2001). Secondly, current measurements (Yuan *et al.* 1995) indicated a deep southwestward flow at a depth of 1900 m near the continental slope southeast of Okinawa Island in winter, whereas the current direction was northeastward 50 km further offshore at 2000 m depth from the end of November 1991 through to the end of summer 1992. Furthermore, at greater depths at the same location, the flow was found to be southwestward from mid November 1991 through to early September 1992. Recently, Ichikawa *et al.* (2000) have reported direct observations of the Ryukyu Current southeast of Amami-Oshima Island. A year-long current record has shown persistent northeastward flow with a speed of about 0.4 m/s at the depth of ~500 m.

Finally, Lee *et al.* (2000) estimated the seasonal cycle of the Kuroshio transport in the channel between Taiwan and the Ryukyu Islands, at the Kuroshio entry point in the ECS. The transport time series were originally based on 20-month long measurements, but by using the sea level data they were extended up to 7 years. The annual transport cycle was evaluated to be 4-10 Sv with a maximum of 24 Sv occurring in the summer, minimum of 20 Sv in the fall, and a weaker secondary maximum in the winter. According to this estimate, the mean trans-Pacific balance of meridional circulation forced by winds and thermohaline processes at 24° N required an additional mean northward flow of 12 Sv with an annual cycle of ± 8 Sv along the eastern boundary of the Ryukyu ridge. If this estimate of the Kuroshio transport annual cycle in the ECS is correct, then it comes as a surprise in that Feng *et al.* (2000) did not report any annual signal in their moored record of the Kuroshio current in the Tokara Strait during 1992-1996.

Overall, the observations imply that the Kuroshio

current system is very complex in spatial and temporal scales and at least three moored arrays are needed to determine the transport at the ocean western boundary, as envisaged by the ongoing Kuroshio Observation Program (KOP). Simultaneous measurements of the mainstream Kuroshio in the ECS and the currents east of the Ryukyu's will allow an assessment of the delicate balances between the mainstream Kuroshio and the Ryukyu Current. The observational array east of Kyushu is required for monitoring the seasonal change in the Kuroshio recirculation. The stratification of the recirculation is dynamically important for the western boundary current system, in particular for the Ryukyu Current (e.g. Ostrovskii 2000). The model-based hypothesis about the barotropic and baroclinic transports (Kagimoto and Yamagata 1997) can be verified by process-oriented and carefully planned observations. In the history of oceanography, there have been few examples where observations aimed at the verification of a proposed hypothesis. The KOP is a hypothesis-oriented and model-supported observational program using modern acoustic technology for ocean measurements.

The methods used in the KOP are described in section 2. The feasibility of the KOP, including an assessment of observational errors, is addressed in section 3, and the program is summarized in section 4.

2. Observational surveys

The KOP developed by Frontier Observational Research System for Global Change/ Japan Marine Science and Technology Center (FORSGC/JAMSTEC) aims to assess the barotropic and baroclinic components of the Kuroshio, allowing model results to be verified. The objective of KOP is to monitor the upstream Kuroshio and then to study the variability associated with this current system by assimilating the obtained data into numerical models. The data will be fed into POM, provided by the Japan Coastal Ocean Predictability Experiment Group of Frontier Research System for Global Change (FRSGC), to improve our capability to forecast the downstream Kuroshio. Both direct and indirect observations of the ocean western boundary dynamics will be carried out by the current-meter and Inverted Echo Sounder with Pressure gauge (PIES) moorings, ship-borne Lowered Acoustic Doppler Current Profiler (LADCP), and CTD surveys. These data will be combined to determine the shallow and deep current, temperature, and vertical velocity fields. The field data should be sufficient to resolve the flow structure with mesoscale resolution thereby describing meanders of the currents, current-eddy interaction, and impact of the bottom topography. A regular survey for 5-10 years is needed to capture the seasonal signal.

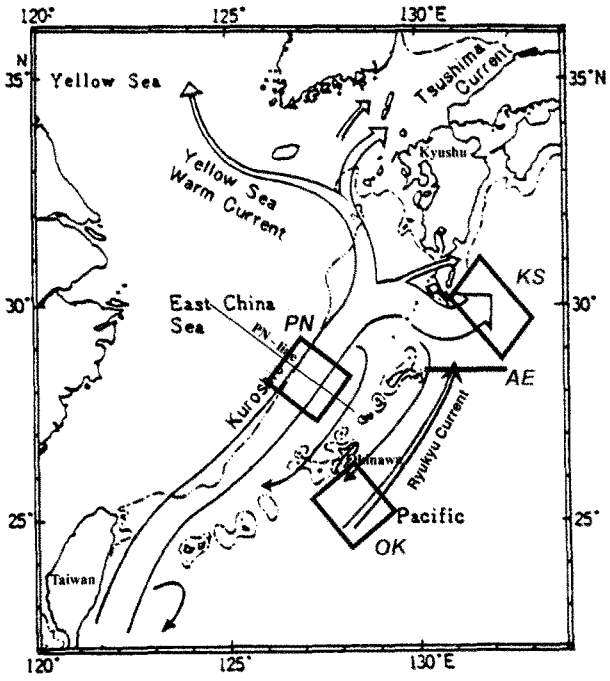

Fig. 1. Schematic map of observational sites. Background - the Kuroshio current system chart (Nitani 1972).

Moored arrays

The goals of KOP are to be achieved by deploying three observational arrays (Fig. 1): 1) in the mainstream Kuroshio in the ECS, 2) in the Ryukyu Current southeast of Okinawa, and 3) east of Kyushu where the Kuroshio, upon exiting the ECS, is joined by the Ryukyu Current. Fig. 2 shows the mooring array southeast of Okinawa. This array is partly operational since November 2000; more instruments are to be deployed in 2001.

The moored arrays are principally composed of PIESs. A PIES measures the abyssal pressure and the round trip time of an acoustic signal travelling between the sea floor and the sea surface (Watts *et al.* 1995). The acoustic travel time can be related to vertical profiles of temperature, salinity, and specific volume anomaly.

The need for two-dimensional coherent arrays of moored instruments is due to the meandering nature of

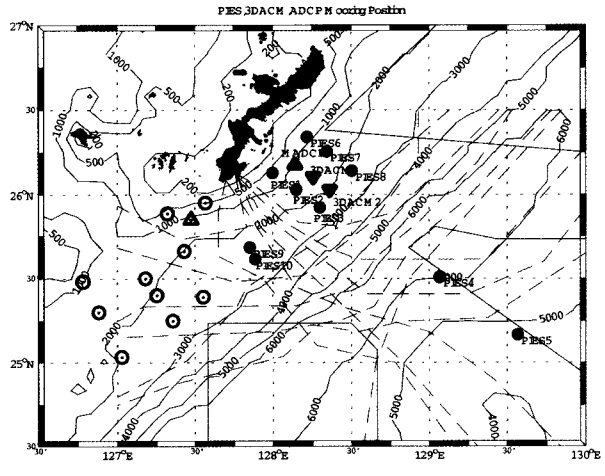

Fig. 2. The KOP mooring array east of the Okinawa Islands. The circles and triangles indicate the PIES and current meter moorings. Filled circles and triangles show moorings deployed in 2000. Empty symbols show new moorings to be deployed in 2001.

the Kuroshio. In particular, meanders have been observed in the ECS with periods of 7 to 23 days and wavelengths of 100-350 km travelling downstream at 8-22 km/day (see Sugimoto *et al.* 1988; Qiu *et al.* 1990; Ito *et al.* 1995; James *et al.* 1999 among others). The fact that the Kuroshio is unstable undermines previous attempts to quantify its transport from an individual hydrographic survey along any single section across the Okinawa Trough.

The two-dimensional arrays of moored instruments should measure density and current structure with mesoscale resolution. It is desirable to maintain a coherent array of PIES moorings, in which neighbouring PIESs are separated by a distance not much greater than the spatial correlation scale, which is a function of the internal Rossby radius, estimated to be about 40 km around Ryukyu Islands (Emery *et al.* 1984).

The moored arrays allow us to observe the eddy-current interactions. The eddy impact is particularly important for the dynamics of the Ryukyu Current. For example, recently, it has been suggested (Yang *et al.* 1999) that the interactions of the Kuroshio with mesoscale eddies east of Taiwan result in a leakage of Kuroshio waters east of Ryukyu/Nansei Islands. Satellite altimeter observations indicate that cyclonic and anticyclonic eddies impinge on the region east of Taiwan at intervals of about 100 days. The sea level difference across the East Taiwan Channel, which indicates the volume of the Kuroshio throughflow, appears to vary coherently with the arrival of the eddies: an approaching anticyclonic (cyclonic) eddy results in higher (lower) sea level difference. Perhaps, the marginally low transport of the Ryukyu Current in late May 1985 (Bryden *et al.* 1991; Yuan *et al.* 1998) was a result of mean flow-eddy interactions east of Taiwan. In situ observations, more frequent than quarterly measurements, are needed to resolve the secular variability of the Kuroshio transport due to current-eddy interactions.

So far the best estimates of the Kuroshio transport in the ECS, are averages of snapshots obtained from geostrophic calculations at a few sections across the Okinawa Trough on a quarterly basis over several years (Fujiwara *et al.* 1987; Ichikawa and Beardsley 1993). These estimates indicate the baroclinic velocities (i.e. the flow associated with lateral variations in density) relative to an assumed level of zero velocity. Bryden *et al.* (1991) examined the referencing geostrophic calculations versus the acoustic Doppler velocity measurements over the Okinawa Trough, southwest of Okinawa Island. Substantial differences between these two types of the observations were documented in regions shallower than 1000 m. The problem with geostrophic estimates of the Kuroshio transport is that the core of the current is often positioned near the shelf break in the ECS and the flow near the bottom may be ageostrophic over this shallow region. Direct measurements of the deep currents are needed to assess the variability of the barotropic component of the flow.

The KOP has envisaged the deployment of a near-bottom three-dimensional acoustic current meter (3DACM) mooring at the center of "triangle" or "square", formed by a set of three or four neighbouring PIESs (Fig. 2). The 3DACM, placed about 100 m above the bottom outside the boundary layer, can not only measure the barotropic current but also be a reference of the baroclinic current calculated from PIESs and CTD data. The upward looking moored acoustic Doppler current profiler (ADCP) will be used over the continental slope region where it will be advantageous to have current profiles for referencing the PIES observations.

In the ECS, the current measurements are important near the shelf break where the Kuroshio axis is often positioned. Doppler velocity profilings indicate that the northward current is 100-150 km wide with a maximum velocity of about 0.8 m/s in the top 100 m layer in

the central ECS (Kaneko *et al.* 1990, 1993; Ito *et al.* 1995; James *et al.* 1999). The current axis tilts offshore with increasing depth. The maximum depth of the Kuroshio is found to be 600-800 m. The northward flow weakens with depth and vanishes a few hundred meters above the bottom of the Okinawa Trough. A deep countercurrent, in the near-bottom layer along the continental slope, in the central ECS has been observed (Ito *et al.* 1995). The velocity of this countercurrent was about 0.2 m/s.

Since fishery trawling, down depths of 600 m, is common practice in the ECS, conventional taut-wire current meter mooring lines cannot be deployed near the shelf break. Instead, it is planned to deploy the trawl-resistant ADCP. Such instruments are bottom mounted with the ADCP positioned inside the bottom mount so that the ADCP cannot interfere with the trawls. Recently, this technique has been successfully used for measuring a branch of the Kuroshio in the Tsushima Strait (Perkins *et al.* 2000).

The overall design of the two-dimensional moored array focuses on measuring the absolute geostrophic current. Such instrumentation has been successfully used for measurements in the Gulf Stream (Shay *et al.* 1995; Watts *et al.* 1995; Hallock and Teague 1995), the downstream Kuroshio (Book 1998), and other basins. A similar observation in the Tsushima Current branch is underway in the Japan/East Sea.

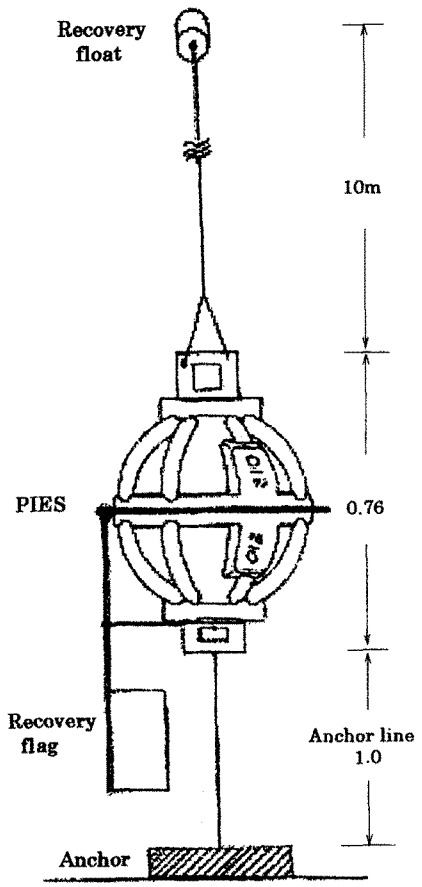

Fig. 3. Sketch of PIES mooring.

The PIES measurements

The KOP takes advantage of various ocean acoustic techniques: PIES, ADCP, and 3DACM. The main observational tool is the URI-GSO PIES 6.1 (hereafter PIES) of the University of Rhode Island (URI) (IES 1999). It is briefly introduced in this subsection.The PIES is an ocean bottom-moored instrument that combines the echo sounder, data-logger, pressure sensor, and acoustic release (Fig. 3). It is moored on a short mooring line, only 1 m above an anchor. The PIES is entirely self-contained in a single 17″ glass sphere and does not require additional buoyancy for recovery. The instrument has the capacity to operate at maximum depths of 6700 m. It features a 32-bit microcontroller that maintains high-performance data manipulation and low-power operation modes, and the data are stored on removable PCMCIA memory cards. Acoustic release and data logging are independent, with a separate release battery. The 17″glass sphere allows for a Lithium battery of the 5-year lifetime.

The PIES measures the vertical acoustic travel time between the sea floor and the sea surface. It transmits 24 pings per hour in programmable bursts of 4, 8, 12, and 24 pings each. The ping interval alternates between 16 and 18 s to avoid aliasing by surface waves. The ping duration and frequency are 5 ms and 12 kHz, respectively. A multi-stage, hard-limiting receiver followed by broad and narrow banded filters, with a noise adaptive detection threshold, provides an echo detection with a time resolution of 0.01 ms for each ping.

The Paroscientific Digiquartz 410 K pressure gauge, which is used in the PIES, has resolution better than 0.002 dbar for a 4000 dbar sensor and a low long-term drift, typically 4 ppm per month.

The PIESs are moored for one to three years. After deployment, the precise position of the PIES is measured by an acoustic monitoring unit, which receives signals from the PIES at various locations around the

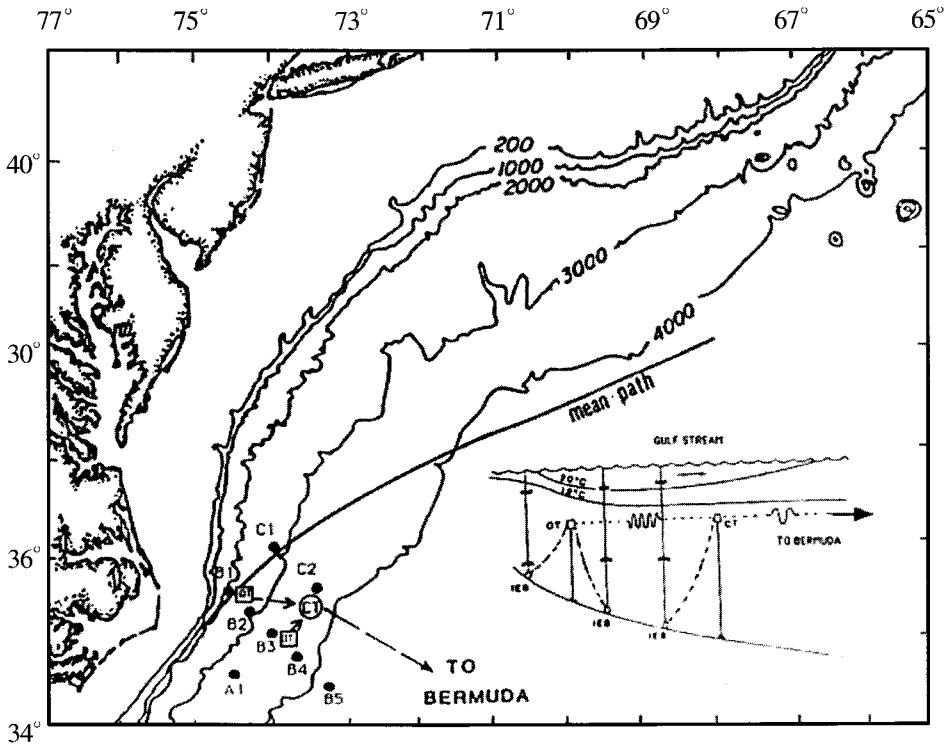

Fig. 4. Location of the IES and transponder moorings. The inset is a schematic of the data relay system (Howden *et al.* 1994).

deployment site. The recovery of the PIES is simple partly due to its radio beacon and flasher.

Hydrographic survey

The moored arrays are to be complemented with CTD surveys that are extensions of existing hydrographic sections along the PN- and OK-lines but with a higher spatial resolution. The expandable bathythermograph and expandable CTD surveys (XBT/XCTD) are supplementary. A CTD probe used in the KOP is mounted with the LADCP.

Repeat observation of ocean currents by a self-contained LADCP (Firing and Gordon 1990; Hacker *et al.* 1996) are made at various locations on the PN- and OK-lines 2 times a year. The LADCP, with a frequency of 150 kHz, can measure the horizontal components of the velocity with a depth bin of 8 m through the whole water column. The absolute velocities for the entire depth are estimated by integrating the velocity shear of horizontal velocities, in which the near-bottom absolute velocities are used as integration constants.

Acoustic data acquisition system

The KOP reflects on the important trend in modern physical oceanography towards the development of an acoustic monitoring system that dramatically extends deployment times, and reduces both maintenance turnaround and ship time costs, while the data are obtained in real-time, thereby substantially improving the predictability of ocean processes. Real-time monitoring can be accomplished via acoustic telemetry of the data or acoustic digital communication link.

Acoustic data telemetry system

A data telemetry option is available for the PIES. A simple acoustic telemetry system for PIES was developed at URI in the late 1980s and was used for obtaining real-time data from IESs in the North Atlantic during August 1989-August 1990 (Howden *et al.* 1991, 1994). The travel time, τ, measured by the IES, was telemetered on a daily basis from 5 IESs in the Gulf Stream off Cape Hatteras to the intermediate transponders at a mid-sound-channel and was then retransmitted to a distant

shore-based receiving station on Bermuda (Fig. 4). The intermediate transponders received the telemetered signals from the IESs and, after stepping down to low frequency, transmitted the telemetered signals to the base station.

The telemetry scheme encoded τ as a time-delayed broadcast acoustic signal relative to some reference time. In other words, the delay of the time of the signal broadcast, with respect to a reference signal, was proportional to the data value τ. For quality control, the telemetered data was also stored in the IESs.

The system was used for real time tracking of the Gulf Stream. From the received data, a daily time series of the depth of the 12°C isotherm, over each IES, which is a proxy for the main thermocline depth, was calculated. The position of the Gulf Stream Wall through the IES array was calculated on a daily basis from the thermocline depth information at each site (Howden *et al.* 1994).

The KOP real-time monitoring is feasible through the telemetry system in the regions where a mid-depth sound channel exists, such as near Okinawa. The system should feature the intermediate transponders moored at the depth of the sound channel and the shore-based receiving station that could be located at Okinawa. The telemetry system can also be used to transmit data to ship. A ship operating near the mooring site can communicate with the PIES through the acoustic telemetry and acquire the data stored. This telemetry concept can be used with other instruments such as current meters and moored ADCPs. At present, the telemetry method is under revision, targeting substantial improvement of the method performance (G. Chaplin, personal communication).

Underwater Acoustic Communication System (UACS)

Another solution for transferring data from a bottom moored instrument and reprogramming its mission is provided by the Underwater Acoustic Communication System (UACS) developed by Kuryanov *et al.* (personal communication) of P.P. Shirshov Institute of Oceanology, Moscow. The UACS is designed to add digital acoustic communication capability to various underwater devices. The core of the system is a digital module with burned-in proprietary signal processing software (Fig. 5). The UACS includes an amplifier and ceramic transducer for receiving and transmitting commands and data between two or more underwater devices. It can be also used for the estimation of the propagation time and impulse response function of the ocean sound channel.

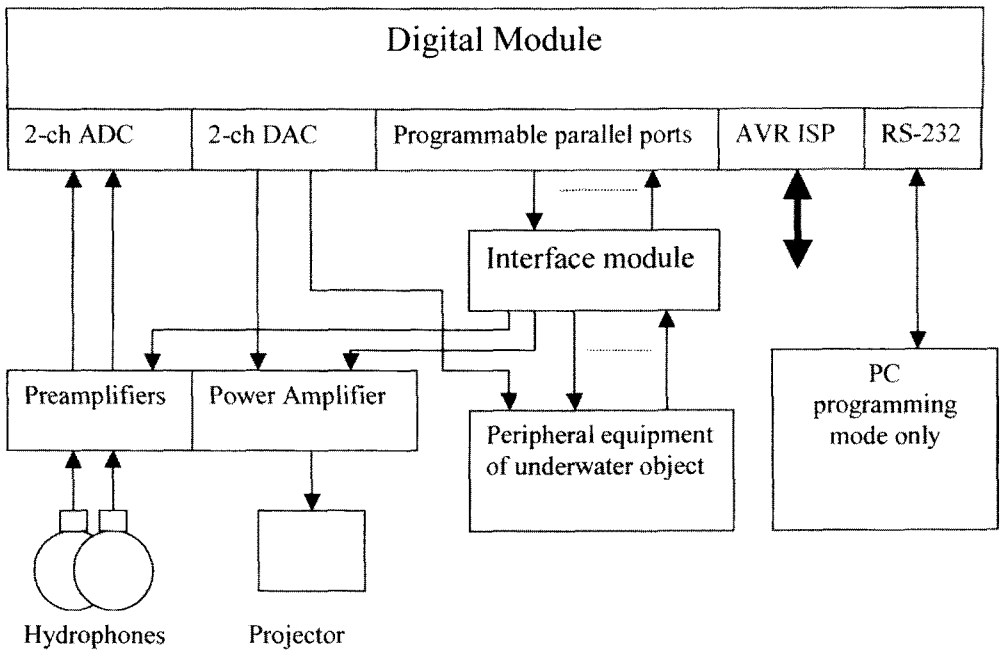

Fig. 5. Block diagram of typical UACS application.

The UACS can be reduced to a digital module only connected to the input/output of the available hydroacoustic channel on PIESs that are already equipped with a hydroacoustic transceiver. The hardware of the digital module is a Printed Circuit Board (PCB) with two processors: Digital Signal Processor (DSP) and RISC processor. The digital module has five operating modes: boot-loading, programming, low-power, transmitting, and receiving modes.

The data processing is based on a pseudo-noise signal communication technology. It was repeatedly and successfully tested with real signals in conditions typical for hydroacoustic communication systems, such as the multi-ray propagation, the Doppler effect, and a high noise level. An additional advantage of this technology is the possibility of parallel processing of the signals from several underwater devices. The UACS can transmit information to another UACS at an optimum rate of 100 bytes per sec, over as long as 10-15 km; the maximum operating range is about 50 km at 1 byte per 10 sec.

A piezoceramic transducer is optional and suitable for underwater communication for a device such as 3DACM, which does not have its own hydroacoustic channel. The piezoceramic transducer works as a transmitter of hydroacoustic signal in the transmitting mode and as a receiver in the receiving mode.

Monitoring the atmospheric forcing and the sea surface

As envisaged by the KOP, monitoring the atmospheric forcing is to be achieved by the combination of remote sensing techniques. The surface wind field at the basin scale can drive the subtropical gyre including the Kuroshio current system. The variation of the surface wind is evaluated by means of the microwave scatterometery provided by SeaWinds on QuikSCAT satellite. The wide swath of scanning allows 92 % of the global ocean to be covered daily (Liu *et al.* 2000). The validation of the wind vectors at each wind vector cells reveals that QuikSCAT can measure the sea surface wind with rms difference of 1.4 m/s by speed and 18 degrees by direction. An integration of the observations is achieved by the objective analysis (Levy and Brown 1986).

Separation of barotropic and baroclinic component by use of the PIES and altimetry data hinges on how correctly one can remove the steric height variations above the seasonal thermocline. The precise estimation of surface heat flux is needed to detect small sea level variations due to the barotropic component of the flow. Moreover, precise knowledge of the temperature field in the mixed layer is also necessary for the PIES data processing. Since conventional methods of the IES data analysis cannot handle variations well above the seasonal thermocline, correct estimation of the air-sea heat flux would be important (Book 1998).

The buoyancy and dynamical forcing at the sea surface can locally affect the mixed layer processes near the Kuroshio. Observational studies reported that the turbulent heat flux near Ryukyu Islands could rise to 660 Wm^{-2} (Garratt and Hyson 1975) and could vary 300 Wm^{-2} within a month (Kondo 1976) in winter. The extraordinary strong cooling and the wind stress at the sea surface, which should dominate the thermal structure in the upper ocean, can be monitored with combined use of the satellite sensors (Liu *et al.* 1988; Konda *et al.* 1996; Schulz *et al.* 1997). The successful monitoring of the surface forcing would provide a knowledge on three-dimensional thermal structure over the KOP region.

Since the KOP's final goal is to improve predictability of the Japanese coastal ocean conditions, it would be eventually necessary to understand an impact of the Kuroshio current system on the coastal phenomena and also the sources of the variations in the KOP area. Use of altimetry data to spatially extended monitoring is the most practical and effective solution. In fact, by the use of the satellite altimetry, variations near the Nansei Islands have recently been revealed to be strongly correlated with the variations of the Kuroshio in the Tokara Strait and coastal temperature in the Bungo Channel (Ichikawa 2000; Ichikawa and Kaneda 2001). Also, the baroclinic Rossby wave propagating from the east, as revealed by the altimetry data, should have an impact on the Kuroshio current system. Akitomo *et al.* (1996) found relationship between the variation of the Kurohiso transport and changes in the depth of the thermocline propagating westward from the east. Latif and Barnett (1996) suggested that the decadal variability of the Kuroshio is affected by the baroclinic Rossby waves generated in the eastern North Pacific.

The altimetry data are also useful for the separation of barotropic and baroclinic components of the PIES observations (Wimbush *et al.* 1997; Book 1998). Especially in the KOP, some of PIESs are planned to be deployed along a TOPEX/POSEIDON track to make it possible to

link the observations of vertical acoustic travel time and bottom pressure with the sea surface height measured from the satellite. Therefore, a link between the bottom pressure data and the sea surface height can be established, which will be useful to handle the pressure data of the other PIESs away from the TOPEX/POSEIDON track. In addition, wide coverage of the altimetry observation will allow us to study differences of phase propagation speeds for barotropic and baroclinic signals.

3. Feasibility Study

In order to ensure that the data obtained by the PIESs would be reliable for the KOP, a feasibility assessment was carried out based on the reanalysis of historical hydrographic data and a test field experiment in the ECS. The PIES measures the time, τ, required for an acoustic pulse to travel from the sea bottom to the surface and back. The travel time, τ, depends primarily on the thermal structure of the water column, and consequently τ fluctuations can be interpreted as fluctuations of dynamic height, heat content, and the depth of the main thermocline due to this relationship (Watts and Rossby 1977). In this feasibility study, we focus on the relationship between t and the water column stratification, and determine whether a relationship does exist between them. It is hoped that these results will help KOP in the final positioning of the PIES arrays and the calibration of the instruments.

Inferring Dynamic Height Anomaly from Acoustic Travel Time

Watts and Rossby (1977) concluded that τ and the dynamic height anomaly, ΔD, are approximately linearly related by Eqn. (1) in many ocean regions when the temperature - salinity (T-S) relationship is tight.

$$\Delta D = -m\tau. \qquad (1)$$

As a result, this relationship allows ΔD to be directly computed from τ if the coefficient m is known. This is the main principal of the IES.

The coefficient m depends on the T-S characteristics of the local area and varies from region to region. This variability has been studied by several authors. For example, Trivers and Wimbush (1994) investigated the spatial variability of m for the North Atlantic, and James and Wimbush (1995) for the Pacific Ocean. Although the study by James and Wimbush (1995) included the ECS, the estimates were obtained on a 5° by 5° grid, which is too coarse to assess the feasibility of KOP. Therefore, a more detailed analysis is required.

The main purpose of such a study is to look at the relationship between τ and ΔD with as fine a resolution as possible and to test whether the relationship in (1) holds for the study area. We examine the variability of m for the north Pacific subtropical gyre between 20°N to 40°N and 120°E to 140°E using historical hydrographic data, at a resolution of 0.5° by 0.5°.

Historical hydrographic data set

The data for the study is derived from historical hydrographic data for the region 20°N-40°N, 120°E-140°E. Several data sources have been used in order to ensure the best possible data coverage. The primary data source is World Ocean Atlas (WOA) 1998 data (www.nodc.noaa.gov/OC5/wod98.html), consisting of standard level CTD and bottle data, and observed level CTD data. The time period extends from 1950 to

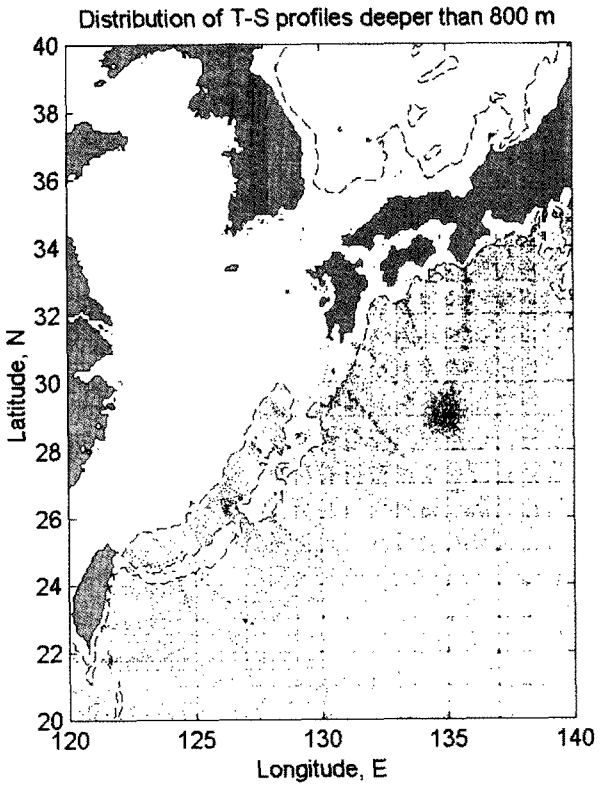

Fig. 6. Distribution of the historical hydrographic observations deeper than 800 m in the northwestern Pacific.

1995. The WOA 1998 data makes up over 60 % of the final data set. CTD data from Japan Oceanographic Data Center (JODC) and World Ocean Circulation Experiment (WOCE), which are not included in WOA 1998, are also used. The JODC and WOCE data run up to 1998. Finally data from the Global Temperature Salinity Profile Program (GTSPP) and Japan-China Co-operative Study of the Kuroshio are also included.

Only observations deeper than 800 m are considered and their distributions have been looked at in some detail. Both the temporal and spatial distributions are variable. Some areas such as the Kuroshio region have very dense coverage, while other regions have limited coverage. Fig. 6 shows the distribution of profiles.

The paucity of data in some regions poses an important problem for the computation of m, since ideally twenty or more profiles are required per grid box in order to obtain a reliable value of m from the regression. As a result, the 0.5° boxes have been merged into 1° by 1° boxes in some cases to improve the map of m. It had been hoped that it would be possible to study the seasonal variability of m but there are not sufficient data. However, any individual grid box with enough data has been looked at.

Method

The acoustic travel time measured by an IES can be defined as

$$\tau = 2 \times 10^4 \int_0^{pj} 1/\rho g c \, dp, \qquad (2)$$

and the dynamic height anomaly as

$$\Delta D = 10^3 \int_{pi}^{pj} \delta \, dp, \qquad (3)$$

where δ is specific volume anomaly (m^3/kg), ρ is density (kg/m^3), g is acceleration due to gravity, and c is sound speed (m/s).

The original hydrographic data was a combination of observed level (T, S, and p) and standard level (T, S, and depth) data. Density was calculated using UNESCO's equation of state (UNESCO 1981) and sound speed was computed from Del Grosso's algorithm (Del Grosso 1974). In the case of standard level data, depth was converted to pressure using Fofonoff and Millards algorithm but with constant gravity (He 1993). This method was chosen as He (1993) concluded that it gave the best results.

The values of τ and ΔD were computed from the historical data by linear integration to a chosen deep pressure limit, p_j. Previous studies have chosen different integral limits to ensure the best possible relationship between τ and ΔD and, thus, a more reliable value for m (Watts and Rossby 1977; Chiswell *et al.* 1986; Wimbush *et al.* 1990). This will be discussed in more detail in the next subsection.

Linear regression of ΔD with τ provided an estimate of the coefficient m. The Signal-to-Noise Ratio (SNR) was also computed as in Eqn. (4) (James and Wimbush 1995). It is calculated from the correlation coefficient, r, between τ and ΔD and indicates the reliability of the fit.

$$SNR = -5\log_{10}(1-r^2) \qquad (4)$$

James and Wimbush (1995) stated that if SNR > 3.61 dB (i.e. $r < -0.9$), the estimate of m was excellent. If 2.22 dB < SNR < 3.61 dB (i.e. $-0.9 < r < -0.8$) then m was good. Any value below 2.22 dB was deemed unreliable.

Mapping m and SNR

The integration limits in Eqns. (2) and (3) were chosen after careful consideration. The number of deep profiles in the historical data set was quite limited, with the number of profiles available decreasing with increasing depth. Since computations of m require as many profiles as possible, the lower pressure limit, p_j, was set to 800 dbar. To ensure that 800 dbar was suitable, values of m were also computed for p_j = 1000 dbar and p_j = 2000 dbar, where possible, to see if there was any variation in m and SNR. The average variation of m was negligible when the integral range was increased, indicating that m had little dependence on the integral range deeper than 800 dbar. Therefore, given that this variation was small, 800 dbar was chosen. This lower limit has in fact already been used in IES studies for this region (Wimbush *et al.* 1997).

The ΔD upper limit, p_i, of 100 dbar was chosen as it gave the best correlation, between ΔD and τ, during tests. Four different upper limits were investigated; 0, 100, 200, and 400 dbar and in the majority of cases, 100 dbar yielded the most reliable estimate of m. The reason for this may be due to the removal of salinity effects in the upper ocean by not integrating from the surface. In summary, values of m and SNR were computed from $\Delta D_{100\text{-}800}$ and $\tau_{0\text{-}800}$.

During the computation of m, the reliability of the

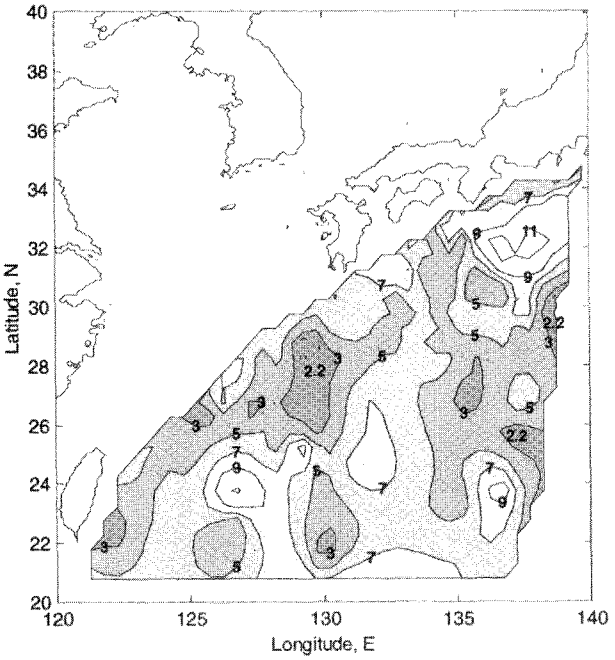

Fig. 7. Signal-to-noise ratio (dB) of the estimate of the linear regression coefficient m.

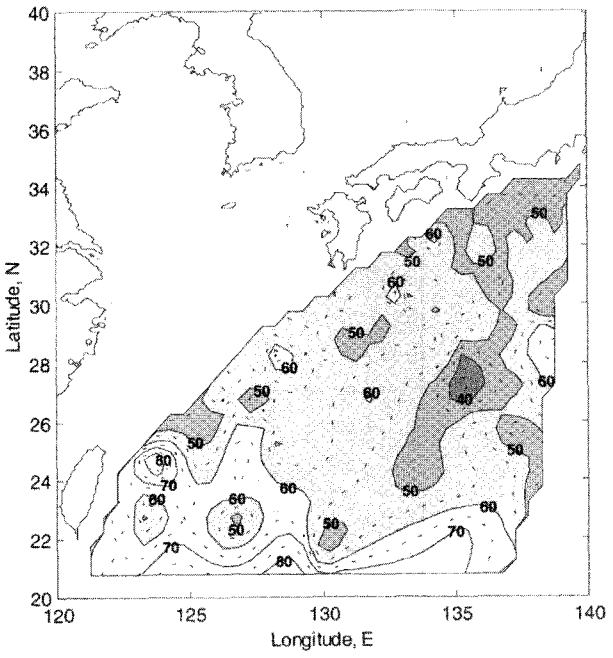

Fig. 8. The linear regression coefficient m (dyn m/s) between $\Delta D_{100\text{-}800}$ and $\tau_{0\text{-}800}$.

estimate was judged by the SNR estimate. In total, over three quarters of the data had SNR greater than 3.61dB. To produce the final maps, m and SNR were interpolated and contoured (Figs. 7 and 8). Care must be taken when analyzing these maps since the coverage of actual data is very poor in some areas.

Fig. 7 shows the contours of SNR for the hydrographic data and Fig. 8 shows the map of m. Excellent estimates of m are found along the southeastern coast of Japan and in the Philippine Sea, east of Taiwan according to Fig. 7. Poor estimates are found northwest of Okinawa and in isolated areas of the Philippine Sea.

James and Wimbush (1995) remarked on the high levels of SNR in the Kuroshio and its extension, concluding that the strong signal in this region ensures a very tight relationship between τ and ΔD. Our result then confirms that IESs are suitable for the KOP mooring sites and would produce excellent and reliable results of ΔD, which could in turn be interpreted as other parameters. There were only a couple of isolated areas of poor SNR and neither of the areas is located at the proposed array sites.

As well as the problem of the paucity of data, the maps could be biased by seasonal changes since m was calculated using all data regardless of season. The subtropical front is known to have very strong seasonal variability (White *et al.* 1978), which may affect m. An attempt was made to look at this problem by studying individual boxes that had sufficient data to compute m for the summer and winter months. Table 1 shows results of the computed summer and winter m values. The investigation revealed no obvious seasonal trend. However, there is a small indication that m increases in summer and decreases in winter over the Kuroshio and Tropical ridges. Aside from this, values of m fluctuated around the climatological mean regardless of season. The reliability of some of these values is questionable since fewer profiles were used to estimate m.

A monthly time series of m was plotted for the approximate region of the proposed PIES site in the ECS (~ 26-28.5°N, 125.5-128.5°E). The data coverage for this area is excellent and so reliable monthly values of m could be estimated. Fig. 9a shows the time series for the anomaly of m. The mean climatological average for this area was 53.33 dyn m/s. The correlation coefficient and the number of profiles used in each monthly computation of m are shown in Figs. 9b and 9c, which helps to interpret the reliability of the m estimates. All values are reliable and there is no obvious seasonal signal as shown in Fig. 9a.

Table 1. Seasonal values of *m* (Summer S=M, J, J, A, S, and Winter W=N, D, J, F, M).

Longitude (Degrees E)	Latitude (Degrees N)	Season	No. Profs.	r	SNR	*m*
128.25	27.75	S	14	-0.96	5.50	63.31
		W	10	-0.97	5.85	68.31
		mean	44	-0.92	4.19	59.05
127.25	28.25	S	28	-0.98	6.89	57.54
		W	18	-0.98	6.60	54.56
		mean	74	-0.97	6.26	54.86
128.75	29.75	S	12	-0.99	12.65	54.73
		W	21	-0.99	9.43	58.91
		mean	35	-0.99	7.96	56.82
123.50	24.75	S	27	-0.94	4.56	86.81
		W	10	-0.94	4.57	81.56
		mean	38	-0.94	4.51	85.12
137.25	21.25	S	13	-0.95	4.94	64.43
		W	15	-0.98	6.81	58.84
		mean	28	-0.96	5.55	61.11
135.25	29.75	S	19	-0.99	8.18	56.92
		W	21	-0.98	7.10	60.50
		mean	65	-0.96	5.51	54.08
137.25	29.75	S	14	-0.99	7.65	54.39
		W	20	-0.99	8.97	53.11
		mean	39	-0.98	7.46	52.21
133.50	29.25	S	15	-0.97	6.44	53.99
		W	11	-0.99	8.32	52.93
		mean	35	-0.97	5.82	51.87
131.25	29.75	S	13	-0.99	10.20	54.08
		W	20	-0.99	9.10	50.99
		mean	43	-0.99	9.37	52.55
132.00	29.75	S	12	-0.99	8.62	54.65
		W	15	-0.98	7.39	41.90
		mean	29	-0.98	7.55	51.82

Distribution of m

The variability of *m* is most likely a direct reflection of the nature of this active western boundary current region. According to Fig. 8, *m* appears to have a complex spatial variability, ranging from 40 dyn m/s to 80 dyn m/s. The most noticeable feature is the region of very high *m* off Taiwan. It is interesting to note that the regions of high *m* off Taiwan coincide with a strong peak of ΔD. However, this relationship is not observed for the documented eddy south of Shikoku. Apart from several cores of variability, the area has average values of *m* ranging between 50 dyn m/s to 60 dyn m/s, with a general tendency for *m* to decrease with distance northeast from Taiwan.

Our values of *m* correspond well with other similar studies. James and Wimbush (1995) reported values of m, computed from hydrographic data, ranging between 50 dyn m/s to 70 dyn m/s. They also observed a maxi-

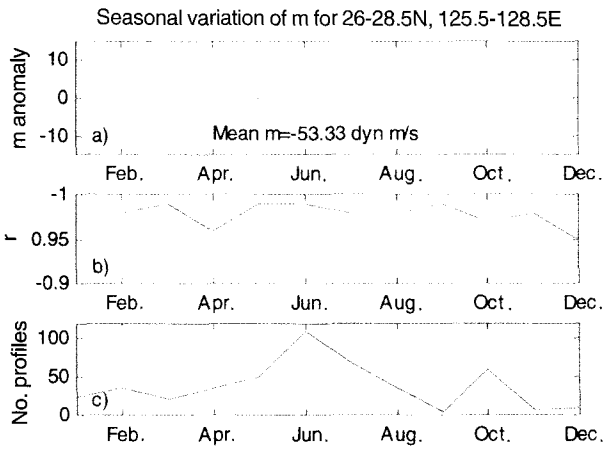

Fig. 9: Time series for the prospective PIES site in the ECS (~ 26-28.5°N, 125.5-128.5°E): a) seasonal variation of m, b) correlation coefficient of m estimate, c) number of profiles used to compute m.

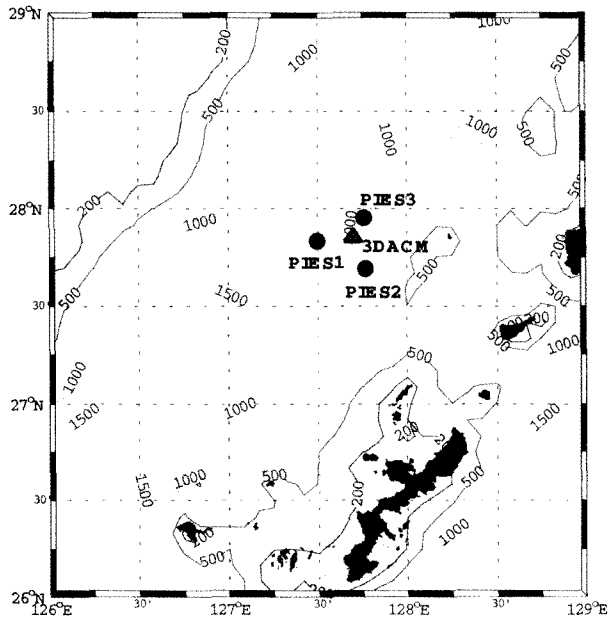

Fig. 10. The KOP test experiment site in the ECS in July-August, 2000. Circles indicate the PIES moorings, triangle - the 3DACM mooring.

mum off Taiwan with m decreasing with distance north-northeast. James *et al.* (1994) reported values of m ranging between 35 dyn m/s to 64 dyn m/s around 28.3°N, 127°E, again similar to our range for m. Wimbush *et al.* (1997) estimated m to be approximately 54.6 dyn m/s from CTD and XBT profiles on the ASUKA line, south of Shikoku.

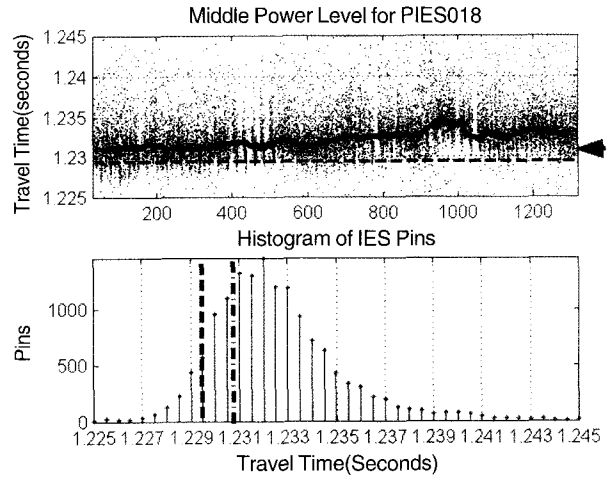

Fig. 11. (Upper panel) The vertical acoustic travel time, τ, from 937 m to the sea surface obtained by PIES3 (#018). The dots are individual 'returns'. The heavy line plots the median τ. Dash line represents the mean τ computed from available historical hydrographic data within the region of the KOP test experiment $\pm 0.25°$ in the summer. Arrow and dash-dot line represent the estimate of τ obtained from the CTD data at the PIES3 site before recovery.
(Lower panel) Histogram of the vertical acoustic travel time measured by PIES3. Dash line represents the mean τ computed from available historical hydrographic. Dash-dot line represents the estimate of τ obtained from the CTD data at the PIES3 site before recovery.

It is interesting to note that James and Wimbush (1995) made SLACTS (Surface Layer Annual Cycle of Temperature and Salinity) corrections to their data to remove any seasonal signal. This correction is often applied when processing IES data. They recomputed m, and compared it to the original value, and found that the change in m was small, 5 dyn m/s at the most. A similar study by Hallock *et al.* (1989) for the North Atlantic found the annual variation of m to be around 0.4 dyn m/s. This agrees well with results in Fig. 9a, where little seasonal variability was noticed.

A factor that has not been considered so far is the secular variability. White (1975) described a strong secular signal in the baroclinic structure of the subtropical gyre related to the bimodal nature of the Kuroshio path and recent studies have revealed a major climate shift since the late 1970's (Graham 1994; Setoh *et al.* 1999). Given the paucity of data, it is possible that some estimations of m come solely from one year or a group of years and could be influenced by the path modality of the Kuroshio. For example, the reported meander

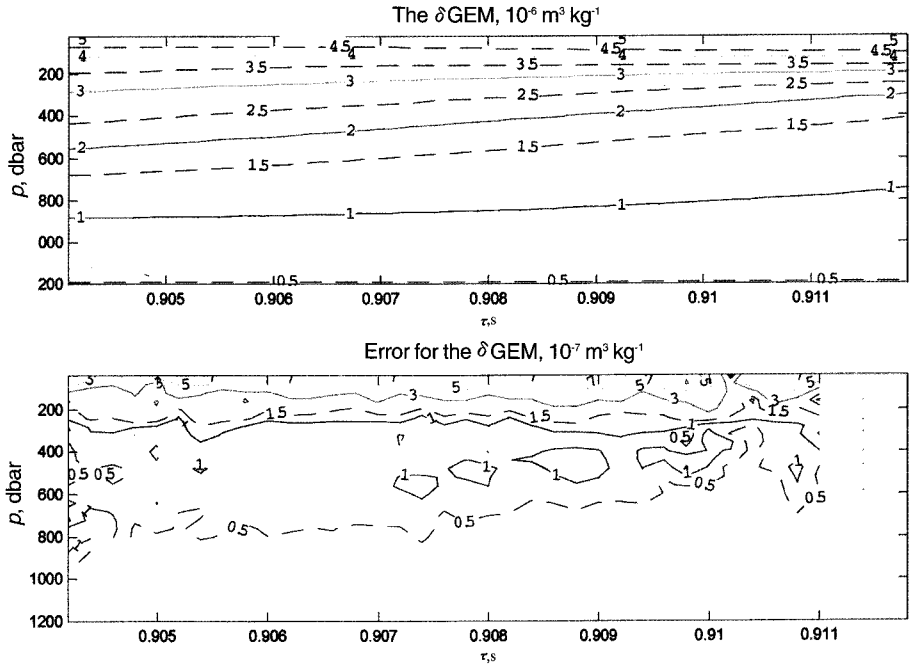

Fig. 12. The upper panel contours the specific-volume-anomaly GEM field fitted to the 448 CTD casts near the PN hydrographic line in the ECS. Contour intervals are 10^{-6} m³/kg (solid line) and $0.5 \cdot 10^{-6}$ m³/kg (dashed line). The lower panel contours the r.m.s. residuals (δ_{CTD} minus δ_{GEM}). Contour intervals are 10^{-7} m³/kg (solid line) and $0.5 \cdot 10^{-7}$ m³/kg (dashed line).

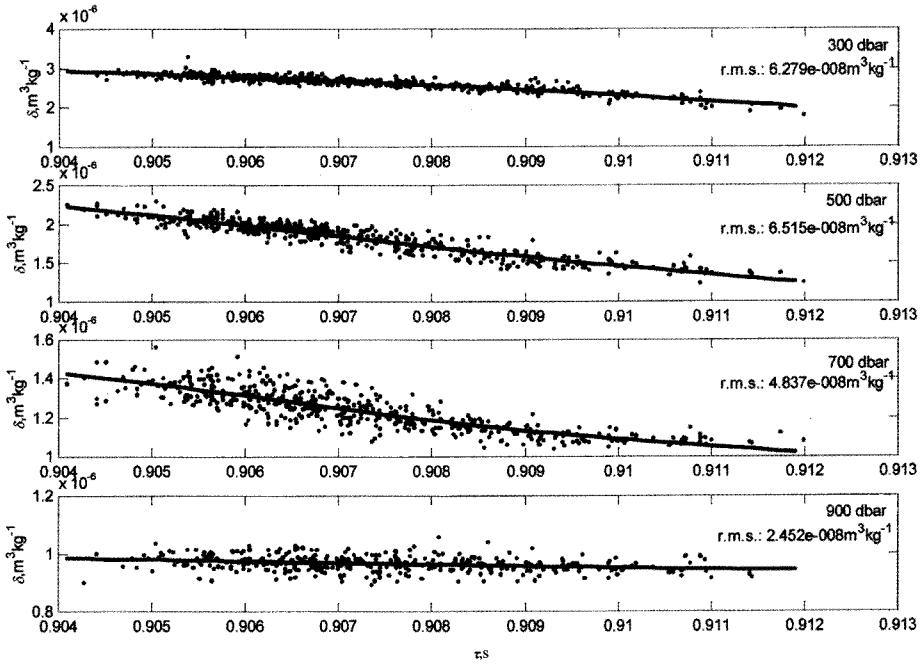

Fig. 13. Scatter plots of δ vs. τ on four representative pressure levels; data are from 448 CTD casts near the PN-line. At each pressure level the δ vs. τ data are fitted by a least-square spline (solid curve).

events in 1953-1955, 1959-1963, 1976-1980, 1982-1984 and 1987-1988 (Qiu and Joyce 1992) may bias the maps.

Test Experiment

Field Operations in the ECS

The FORSGC/JAMSTEC has successfully carried out the KOP test experiment in the ECS. The field operations included three PIESs and one 3DACM mooring, CTD casts, and acoustic telemetry test experiments. The moored array (Fig. 10) operated for almost two months, at depth of about 1000 m, in the ECS during July-August 2000. Three PIESs were deployed on July 2-3, 2000 at the prospective KOP mooring site near the PN-line in the ECS. All three PIES moorings operated normally collecting high quality acoustic and pressure data until their recovery on August 24-25, 2000.

The test experiment data showed that

- The IES signal was good at the mid and low IES power modes, though an early return signal was common (Fig. 11).
- The vertical acoustic travel time, τ, derived with conventional methods of the IES data analysis is consistent with the KOP CTD measurements and the historical hydrographic observations in the area (Fig. 11). The observed round-trip travel time, τ, obtained in the experiment perfectly matches with that computed from the hydrographic data in the feasibility study.
- The telemetry test demonstrated the robustness of the PIES data, with 95 % confidence at distances slightly greater than 2 km and depths of about 1000 m.

Gravest Empirical Mode

To obtain a velocity profile from the KOP test experiment data it is necessary to combine the PIES measurement of τ with the reference velocity from the near-bottom 3DACM. As it will be shown below, τ can be projected onto the vertical specific volume anomaly, δ, profile. By using the time series of δ profiles at two PIESs, the relative geostrophic velocities can be computed at each measurement time. The relative velocities should then be referenced to the near-bottom current meter data.

Recently, Meinen and Watts (2000) developed a technique to represent the vertical and lateral structure of density and temperature by a Gravest Empirical Mode (GEM) that captures most of the variance in the hydrographic data. The mode is "gravest" in the sense that the T and S fields shift vertically throughout the water col-

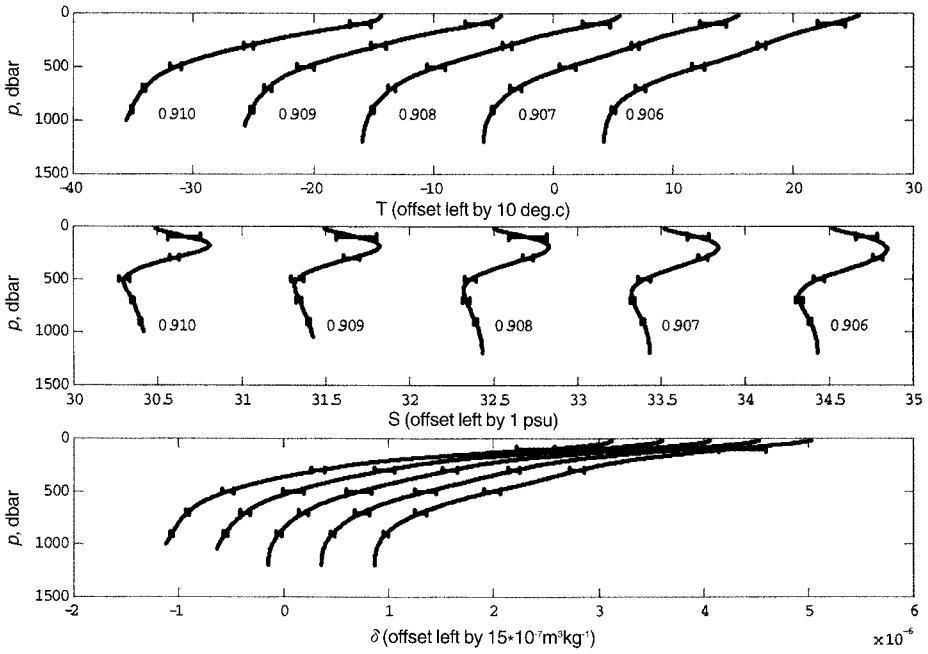

Fig. 14. The variation of the T, S, and δ GEM profiles (the upper, middle, and lower panels, respectively) in the KOP test experiment area. The sets of profiles are plotted at intervals of 1 ms. The error-bars show the r.m.s. residuals.

umn in such a pattern that local isopycnal displacements resemble a "fundamental-mode" (Watts *et al.* 2000). Within the GEM's framework, two-dimensional fields of $\delta(p,t)$, $T(p,t)$, and $S(p,t)$ are parameterized by a cubic smoothing spline. The resultant two-dimensional model fields will represent the basic thermohaline features such as the pycnocline depth while the large uncertainties occur in the mixed layer.

The δGEM field for the KOP test experiment site is computed from 448 CTD profiles deeper than 700 m obtained by Nagasaki Marine Observatory during 1987 -2000 along the PN-line. The travel time $\tau_{0\text{-}700}$ is computed for individual profiles. Then the profiles are binned and averaged at 0.2 ms intervals of $\tau_{0\text{-}700}$. The observed two-dimensional fields are fitted by a fourth-order least-square spline (de Boor 1999), as described in Book (1998). The spline approximation requires a knot sequence indicating pressure levels at which the spline was forced through the original value. The knots used here are at 20 dbar in the upper layer and 100 dbar in the range 200-1200 dbar. The smoothing parameter taken from Book (1998), which controls the flexibility of the spline, provides us with a qualitatively adequate fit. Notice that the seasonal correction is not carried out here due to the negligibly small amplitude of the seasonal changes in the upper layer in the KOP test experiment area.

Fig. 12 plots the δGEM field along with errors of the spline fit. The δ GEM field reflects the linear pattern of the vertical shift of the pycnocline in the ECS except for $t > 0.91$ ms. The observations offshore the mainstream Kuroshio reflect a rather simple thermohaline structure below the upper 200 m layer in the ECS. The linear behavior of the δ GEM field in the range 300-700 dbar may indicate swinging of the Kuroshio axis over the continental slope (Sun and Su 1994). Below 200 m, the stratification is largely determined by waters carried by the Kuroshio, and to a lesser extent by intrusions of the Subtropical Mode Water and the North Pacific Intermediate Water into the ECS through the straits in the Ryukyu Ridge, in particular, the Kerama gap throughflow (Morinaga *et al.* 1998).

The r.m.s. of the δ GEM fit errors, ϵ, is high and more than 10 % throughout the upper 200 m layer. The uncertainties ϵ decrease through the seasonal thermocline to 5 % at 400-600 m. It should be noted that these estimates are based on a large number of CTD samplings in the range $0.905 < \tau < 0.91$ ms as is evident in Fig. 13.

The GEM model is also fitted to the T and S data. As was shown by Watts *et al.* (2000), the GEM exhibits how greatly the vertical profiles of T, S, and δ change as a function of τ. Fig. 14 plots the composites of the curves corresponding to a set of the τ-values at every 1 ms intervals. The horizontal error bars are the r.m.s. misfits from the respective GEM fields. Fig. 14 shows that the GEM realistically captures the basic salinity structure, which is persistent in the ECS all year round. This persistent subsurface salinity maximum is maintained by the North Pacific Tropical Water carried by the Kuroshio. The salinity minimum due to the North Pacific Intermediate Water varies between 500 m and 650 m, implying a large variation in the intermediate water supply due to the swinging of the Kuroshio axis west of the KOP test area in the ECS.

Following Book (1998), the relative velocity can be calculated by using the geostrophic method from the δ GEM time series of PIES pairs. The GEM relative velocity profiles are then referenced to the absolute velocities measured by the 3DACM.

Overall, the GEM technique proved to be useful for interpreting the PIES test measurements. It took advantage of the purely empirical description of the dynamical structure of the Kuroshio current system in the ECS. While capturing the most of the variability, it seeks a basic state that is stable in the τ space i.e., it can be time dependent. It is suited for the ECS region where the mainstream Kuroshio swings and the Kuroshio Countercurrent can develop. By using the δ GEM model, it is possible to reconstruct the time series of the current, temperature, and salinity fields and hence time varying volume, heat, and fresh water transports.

4. Summary

A major objective of KOP is to understand the barotropic and baroclinic components of the Kuroshio. This new knowledge is, then, used to verify and improve our modeling capability of the Japanese coastal waters with a major focus on understanding the seasonal and interannual components of the current.

A long-term measurement array is being built up on either side of Okinawa and east of the Tokara Strait. The field program consists of intensive measurements by ADCPs, 3DACMs, CTD, XBT/XCTD, and PIESs that will be combined with satellite altimeter data. The basic surveys are essentially extensions of existing

hydrographic sections across the Kuroshio, near Okinawa, but with more frequent observations and with better spatial resolution and a strong emphasis on the use of oceanic acoustic techniques.

Three two-dimensional moored arrays of 10-20 PIESs each will, for the first time, allow daily monitoring of the major components of the Kuroshio current system with mesoscale resolution. From these maps, it is hoped that KOP will be able to determine the time-varying mass and heat transports of the Kuroshio and Ryukyu Current, observe the interaction of the currents with mesoscale eddies, and better understand the physics of the Kuroshio instabilities. The observational system targets real-time monitoring via acoustic underwater communication. The system will be implemented to transfer the data to ship or surface buoys, or listening station on Okinawa. It will dramatically reduce operational costs and risks during recovery and redeployment.

The feasibility study shows that PIES can be used in the Kuroshio current system, confirming its suitability for the KOP. ΔD estimated from observed τ will produce instructive results for improving the Japanese coastal ocean predictability. The linear relationship between τ and ΔD is excellent in the upstream Kuroshio region. Yet, spatial and temporal variability of the linear regression coefficient, m, should be considered by KOP when calibrating the PIES. It is advisable to determine m from in-situ CTD profiles at each local PIES site rather than use the regional averages estimated here, but the feasibility study serves as a useful tool for comparison of the results. The location of the arrays satisfies requirements derived from this analysis.

The KOP test field experiment has been carried out in the ECS over the summer 2000. It demonstrated the robustness of our approach to coastal water monitoring. The reliability of the PIES and 3DACM measurements was confirmed through the data inter-comparison and validation from the KOP CTD observations and historical hydrographic data set.

The newly available GEM method is used to relate time τ, obtained from the KOP test PIES data, to vertical profiles of T, S, and δ. This representation defines the temperature, salinity, and specific volume anomaly fields as a function of p and τ. Within the GEM framework, the KOP PIES measurements are inverted to give time series of T, S, and δ profiles. This allows an estimation of the geopotential thickness above the PIES. Consequently, geostrophic velocity profiles can be calculated from the lateral gradients of the geopotential thickness between the neighboring PIESs. The relative geostrophic velocity profile is then referred to the KOP 3DACM observations.

The PIES data analysis will allows us to infer the stratification variability in terms of the pycnocline depth and the specific volume anomaly profile. This survey will be very useful in obtaining multiyear time series of the dynamically significant parameters of both ocean stratification and bottom pressure.

Acknowlodgements

We would like to thank Dr. M.-S. Suk and Prof. K. Kim for their reviews.

References

Akitomo, K., M. Ooi, T. Awaji, and K. Kutsuwada. 1996. Interannual variability of the Kuroshio transport in response to the wind stress field over the North Pacific: Its relation to the path variation south of Japan. *J. Geophys. Res.*, 101, 14057 - 14071.

Book, J. 1998. Kuroshio variations off southwest Japan. M.Sc. Thesis, Univ. Rhode Island, 91 p.

de Boor, C. 1999. *Spline Toolbox User's Guide: For use with MATLAB. Version 2.* The Math Works Inc., 108 p.

Bryden, H.L., D.H. Roemmich, and J.A. Church. 1991. Ocean transport across 24°N in the Pacific. *Deep-Sea Res.*, 38, 297-324.

Chiswell, S.M., D.R. Watts, and M. Wimbush. 1986. Using Inverted Echo Sounders to measure dynamic height in the eastern equatorial Pacific during the 1982-1983 El Nino. *Deep-Sea Res.*, 33, 981-991.

Chiswell, S.M. 1994. Using an array of Inverted Echo Sounders to measure dynamic height and geostrophic current in the North Pacific Subtropical Gyre. *J. Atmos. Oceanic Technol.*, 11, 1420-1424.

Del Grosso, V.A. 1974. New comparisons for the speed of sound in natural waters (with comparisons to other equations). *J. Acoustic. Soc. Am.*, 56, 1084-1091.

Emery, W.J., W.G. Lee, and L. Magaard. 1984. Geographic and seasonal distributions of Brunt-Vaisala frequency and Rossby radii in the North Atlantic and North Pacific. *J. Phys. Oceanogr.*, 14, 294-317.

Feng, M., H. Mitsudera, and Y. Yoshikawa. 2000. Structure and variability of the Kuroshio Current in Tokara Strait. *J.*

Phys. Oceanogr., 30, 2257-2276.

Firing, E. and R.L. Gordon. 1990. Deep ocean acoustic current profiling. p.192-201. In: *Proc. Fourth IEEE Working Conference on Current Measurements, Clinton, MD.*

Fujiwara, I., Y. Hanzawa, I. Eguchi, and K. Hirano. 1987. Seasonal oceanic conditions on a fixed line in the East China Sea. *The Oceanogr. Mag.*, 37, 37-46.

Garratt, J.R. and P. Hyson. 1975. Vertical fluxes of momentum, sensible heat and water vapor during the air mass transformation experiment (AMTEX). *J. Meteor. Soc. Japan,* 53, 149 - 160.

Graham, N.E. 1994. Decadal-scale climate variability in the tropical and North Pacific during 1970's and 1980's: Observation and model results. *Climate Dynamics,* 10, 135-162.

Hacker, P., E. Firing, W.D. Wilson, and R. Molinari. 1996. Direct observations of the current structure east of the Bahamas. *Geophys. Res. Lett.*, 23, 1127-1130.

Hallock, Z.R., J.L. Mitchell, and J.D. Thompson. 1989. Sea surface topographic variability near the New England Seamounts: An intercomparison among in situ observations, numerical simulations and Geosat altimetry from the Regional Energetic Experiment. *J. Geophys. Res.*, 94, 8021-8028.

Hallock, Z.R. and W.J. Teague. 1995. On the meridional surface profile of the Gulf Stream at 55W. *J. Geophys. Res.*, 100(C7), 13615-13624.

He, Y. 1993. Determining baroclinic velocity with Inverted Echo Sounders. M.Sc. Thesis, Univ. Rhode Island, 135 p.

He, Y., D.R. Watts, and K.L. Tracey. 1998. Determining geostrophic velocity shear profiles with Inverted Echo Sounders. *J. Geophys. Res.*, 103, 5607-5622.

Howden, S., K. Tracey, D.R. Watts, and H.T. Rossby. 1991. *Inverted Echo Sounder Telemetry System Report.* GSO Tech. Rep. #91-8, Univ. Rhode Island, Narragansett, RI, 39 p.

Howden, S.D., D.R. Watts, K.L. Tracey, and H.T. Rossby. 1994. An acoustic telemetry system implemented for real-time monitoring of the Gulf Stream with inverted echo sounders. *J. Atmos. Oceanic Technol.*, 11, 567-571.

Ichikawa, H. and R.C. Beardsley. 1993. Temporal and spatial variability of volume transport of the Kuroshio in the East China Sea. *Deep-Sea Res.*, 40, 583-605.

Ichikawa, H., H. Nakamura, and A. Nishima. 2000. Observation of the Kuroshio upstream region. *Kaiyo Monthly,* 32, 504-513 (In Japanese).

Ichikawa, K. 2001. Variation of the Kuroshio in the Tokara Strait induced by meso-scale eddies. *J. Oceanogr.*, 57, 55-68.

Ichikawa, K. and A. Kaneda. 2001. Coastal impacts of off-shore meso-scale eddies through the Kuroshio variation. *La Mer* (In press).

Imawaki, S., H. Uchida, H. Ichikawa, M. Fukasawa, and S. Umatani. 1997. Time series of the Kuroshio transport derived from field observations and altimetry data. *International WOCE Newsletter,* 25, 15-18.

Imawaki, S., H. Uchida, H. Ichikawa, M. Fukasawa, and S. Umatani. 2001. Satellite altimeter monitoring the Kuroshio transport, south of Japan. *Geophys. Res. Lett.*, 28, 17-20.

IES. 1999. *IES Model 6.1. Inverted Echo Sounder User Mannual.* URI GSO, Narragansett, RI, 41 p.

Ito, T., A. Kaneko, H. Furukawa, N. Gohda, and W. Koterayama. 1995. A structure of the Kuroshio and its related upwelling on the East China Sea shelf slope. *J. Oceanogr.*, 51, 267- 278.

James, C., M. Wimbush, and H. Ichikawa. 1994. *East China Sea, Kuroshio 1991-1992 Data Report.* Grad. Sch. Oceanogr. Data Report 94-3, Univ. Rhode Island.

James, C. and M. Wimbush. 1995. Inferring dynamic height variations from acoustic travel time in the Pacific Ocean. *J. Oceanogr.*, 51, 553-569.

James, C., M. Wimbush, and H. Ichikawa. 1999. Kuroshio meanders in the East China Sea. *J. Phys. Oceanogr.*, 29, 259-272.

Kagimoto, T. and T. Yamagata. 1997. Seasonal transport variations of the Kuroshio: An OGCM simulation. *J. Phys. Oceanogr.*, 27, 403-418.

Kaneko, A., W. Koterayama, H. Honji, S. Mizuno, K. Kawatate, and R.L. Gordon. 1990. A cross-stream survey of the upper 400 m of the Kuroshio by an ADCP on a towed fish. *Deep-Sea Res.*, 37, 875-889.

Kaneko, A., S. Mizuno, W. Koterayama, and R.L. Gordon. 1992. Cross-stream velocity structures and their downstream variation of the Kuroshio around Japan. *Deep-Sea Res.*, 39, 1583-1594.

Kaneko, A., W. Koterayama, M. Nakamura, S. Mizuno, and H. Furukawa. 1993. Towed ADCP fish with depth and roll controllable wings and its application to the Kuroshio observation. *J. Oceanogr.*, 49, 383-395.

Konda, M., N. Imasato, and A. Shibata. 1996. A new method to determine near-sea surface temperature by using satellite data. *J. Geophys. Res.*, 101, 14349-14360.

Kondo, J. 1976. Heat balance of the East China Sea during the Air Mass Transformation Experiment. *J. Meteor. Soc. Japan*, 54, 382-398.

Kutsuwada, K. and T. Teramoto. 1987. Monthly maps of

surface wind stress fields over the North Pacific during 1961-1984. *Bull. Ocean Res. Inst., Univ. Tokyo*, 24, 1-100.

Latif, M. and T.P. Barnett. 1996. Decadal climate variability over the North Pacific and North America; Dynamics and predictability. *J. Climate*, 9, 2407-2423.

Levy, G. and R.A. Brown. 1986. A simple, objective analysis scheme for scatterometer data. *J. Geophys. Res.*, 91, 5153-5158.

Lee, T.N., W.E. Johns, Ch.-T. Liu, and D. Zhang. 2000. The Kuroshio east of Taiwan - Mean transport and seasonal cycle with comparison to the Florida Current. *J. Phys. Oceanogr.* (revised).

Liu, W.T. 1988. Moisture and latent heat fluxes variabilities on the Tropical Pacific derived from satellite data. *J. Geophys. Res.*, 93, 6749-6760.

Liu, W.T., H. Hu, and S. Yueh. 2000. Interplay between wind and rain observed in Hurricane Floyd. *EOS Trans. AGU*, 81, 253-257.

Meinen, Ch.S. and D.R. Watts. 1998. Calibrating inverted echo sounders equipped with pressure sensors. *J. Atmos. Oceanic Technol.*, 15, 1340-1346.

Meinen, Ch.S. and D.R.Watts. 2000. Vertical structure and transport on a transect across the North Atlantic Current near 42° N: Time series and mean. *J. Geophys. Res.*, 105, 21869-21891.

Mellor, G. 1991. An equation of state for numerical models of oceans and estuaries. *J. Atmos. Oceanic Technol.*, 8, 609-611.

Morinaga, K., O. Kato, N. Nakagawa, and B. Guo. 1998. Flow pattern of the Kuroshio west of the main Okinawa island. p. 203-210. In: *Proceedings of Japan-China Joint Symposium on Cooperative Study of Subtropical Circulation System*, Nagasaki, Japan, 1-4 Dec. 1997. Seikai National Fisheries Research Institute, Fisheries Agency of Japan, Nagasaki.

Nitani, H. 1972. Beginning of the Kuroshio. p. 129-163. In: *Kuroshio - Its Physical Aspects*, eds. by H. Stommel and K. Yoshida. Univ. Tokyo Press, Tokyo.

Ostrovskii, A.G. 2000. On influence of stratification on the Kuroshio recirculation. (submitted).

Perkins, H., W.J. Teague, G.A. Jacobs, K.I. Chang, and M.-S. Suk. 2000. Current in Tsushima-Korea Strait during summer 2000. *Geophys. Res. Lett.*, 27, 3033-3036.

Qiu, B., T. Toda, and N. Imasato. 1990. On Kuroshio front fluctuations in the East China Sea using satellite and in situ observational data. *J. Geophys. Res.*, 95 (C10), 18191-18203.

Qiu, B. and T. Joyce. 1992. Interannual variability in the mid- and low-latitude Western North Pacific. *J. Phys. Oceanogr.*, 22, 1062-1079.

Reid, J.L. 1961. On the geostrophic flow at the surface of the Pacific Ocean with respect to the 1,000-decibar surface. *Tellus*, 13, 489-502.

Sakamoto, T. and T. Yamagata. 1996. Seasonal transport variations of the wind-driven ocean circulation in a two-layer planetary geostrophic model with a continental slope. *J. Mar. Res.*, 54, 261-284.

Setoh, T., S. Imawaki, A. Ostrovskii, and S. Umatani. 1999. Interdecadal variations of ENSO signals and annual cycles revealed by wavelet analysis. *J. Oceanogr.*, 55, 385-394.

Sugimoto, T., S. Kimura, and K. Miyaji. 1988. Meander of the Kuroshio front and current variability in the East China Sea. *J. Oceanogr. Soc. Japan*, 44, 125-135.

Sun, X.-P. and Y.-F.Su. 1994. On the variation of Kuroshio in East China Sea. p. 49-58. In: *Oceanology of China Seas.Vol. 1*, eds. by D. Zhou, Y.-B. Liang, and C. K. Tseng. Kluwer Acad. Publ.

Shay, T.J., J.M. Bane, D.R. Watts, and K.L. Tracey. 1995. Gulf Stream flow field and events at 68W. *J. Geophys. Res.*, 100, 22565-22589.

Schulz, J., J. Meywerk, S. Ewald, and P. Schluessel. 1997. Evaluation of satellite-derived latent heat fluxes. *J. Climate*, 10, 2782 - 2795.

Teague, W.J., A.M. Shiller, G.A. Jacobs, and J.L. Mitchell. 1995. Kuroshio sea surface height fluctuations observed simultaneously with Inverted Echo Sounders and TOPEX/POSEIDON. *J. Geophys. Res.*, 100, 24987-24994.

Trivers, G. and M. Wimbush. 1994. Using acoustic travel time to determine dynamic height variations in the North Atlantic Ocean. *J. Atmos. Oceanic Technol.*, 11, 1309-1316.

UNESCO. 1981. *10th Report of the Joint Panel on Oceanographic Tables and Standards.* UNESCO Tech. Pap. in Marine Science No 3, UNESCO, Paris, 25 p.

Watts, R. and T. Rossby. 1977. Measuring dynamic heights with Inverted Echo Sounders: Results from MODE. *J. Phys. Oceanogr.*, 7, 345-358.

Watts, D.R., K.L. Tracey, J.M. Bane, and T.J. Shay. 1995. Gulf Stream path and thermocline structure near 74° W and 68° W. *J. Geophys. Res.*, 100 (C9), 18291-18312.

Watts, D.R., C. Sun, and S. Rintoul. 2000. A two-dimensional gravest empirical mode determined from hydrographic observations in the Subantarctic Front. *J. Phys. Oceanogr.* (submitted).

White, W. 1975. Secular variability in the large scale baroclinic transport of the North Pacific from 1950-1970. *J. Mar. Res.*, 33, 144-155.

White, H., K. Hasunuma, and H. Solomon. 1978. Large-scale seasonal and secular variability of the subtropical front in the western North Pacific from 1954-1974. *J. Geophys. Res.*, 83, 4531-4544.

Wimbush, M., S. Chiswell, R. Lukas, and K.A. Donohue. 1990. Inverted Echo Sounder measurement of dynamic height through an ENSO cycle in the central equatorial Pacific. *IEEE J. Oceanic Eng.*, 15, 380-383.

Wimbush, M., H. Ichikawa, J. Book, H. Ushida, and H. Kinoshita. 1997. Separating baroclinic and barotropic sea surface height components in the ASUKA region by combining altimeter and Inverted Echo Sounder measurements. p. 33-50. In: *Proceedings Symposium on Ocean-Earth Dynamics and Satellite Altimetry, Tokyo.*

Worthington, L.V. and H. Kawai. 1972. Comparison between deep sections across the Kuroshio and the Florida Current and Gulf Stream. In: *Kuroshio - Its Physical Aspects,* eds. by H. Stommel and K. Yoshida. Univ. Tokyo Press, Tokyo.

Yang, Y., C.-T. Liu, J.-H. Hu, and M. Koga. 1999. Taiwan Current (Kuroshio) and impinging eddies. *J. Oceanogr.*, 55, 609-617.

Yuan, Y., J. Su, Z. Pan, H. Chen, H. Ichikawa, S. Imawaki, K. Kawatate, K. Takano, and S. Umatani. 1995. The western boundary current east of the Ryukyu Islands. *La mer,* 33, 1-11.

Yuan, Y., A. Kaneko, J. Su, X-H. Zhu, Y. Liu, N. Gohda, and H. Chen. 1998. The Kuroshio east of Taiwan and in the East China Sea and the currents east of Ryukyu/Nansei Islands during early summer of 1996. *J. Oceanogr.*, 54, 217-226.

Received Mar. 9, 2001
Accepted Jun. 30, 2001